Proceedings of the 6th International Conference on Gas Hydrates (ICGH 2008), Vancouver, British Columbia, CANADA, July 6-10, 2008.

SEISMIC TIME-LAPSE MONITORING OF POTENTIAL GAS HYDRATE DISSOCIATION AROUND BOREHOLES - COULD IT BE FEASIBLE? A CONCEPTUAL 2D STUDY LINKING GEOMECHANICAL AND SEISMIC FD MODELS

Ingo Pecher*
Inst. of Petroleum Engineering, Heriot-Watt Univ., Edinburgh, EH3 9HP, UK

Reem Freij-Ayoub
CSIRO Petroleum, P.O. Box 1130, Bentley, WA 6102, AUSTRALIA

Jinhai Yang, Ross Anderson, Bahman Tohidi, Colin MacBeth
Inst. of Petroleum Engineering, Heriot-Watt Univ., Edinburgh, EH3 9HP, UK

Ben Clennell
CSIRO Petroleum, P.O. Box 1130, Bentley, WA 6102, AUSTRALIA

ABSTRACT

Monitoring of the seafloor for gas hydrate dissociation around boreholes during hydrocarbon production is likely to involve seismic methods because of the strong sensitivity of P-wave velocity to gas in sediment pores. Here, based on geomechanical models, we apply commonly used rock physics modeling to predict the seismic response to gas hydrate dissociation with a focus on P-impedance and performed sensitivity tests. For a given initial gas hydrate saturation, the mode of gas hydrate distribution (cementation, frame-bearing, or pore-filling) has the strongest effect on P-impedance, followed by the mesoscopic distribution of gas bubbles (evenly distributed in pores or "patchy"), gas saturation, and pore pressure. Of these, the distribution of gas is likely to be most challenging to predict. Conceptual 2-D FD wave-propagation modeling shows that it could be possible to detect gas hydrate dissociation after a few days.

Keywords: gas hydrates, rock physics, seismic modeling, wellbore stability

NOMENCLATURE

FD Finite difference
I Compressional impedance [(km/s)(g/cm^3)]
J Shear impedance [(km/s)(g/cm^3)]
OBS Ocean bottom seismometer
Vp Compressional-wave velocity [km/s]
Vs Shear-wave velocity [km/s]
ρ density [g/cm^3]

INTRODUCTION

Dissociation of gas hydrate to water and potentially overpressured gas around boreholes may constitute a hazard for deep-water hydrocarbon production. Future strategies to mitigate this risk are likely to include monitoring for early detection of dissociation. Seismic methods are particularly promising, largely because of a high sensitivity of P-wave velocity (Vp) to gas in the pore space of unconsolidated sediments [1].

Several groups have conducted geomechanical modeling of wellbore stability during gas hydrate dissociation in recent years [2-4]. We have also embarked on accompanying laboratory experiments [5]. We envisage that monitoring designs will include analyses of the thresholds at which gas hydrate dissociation will be detected. For such analyses, knowledge of the response of sediments to dissociation at specific locations will

* Corresponding author: Phone: +44 131 451 3675 Fax +44 131 451 3127 E-mail: ingo.pecher@pet.hw.ac.uk

be critical, which could e.g., be determined from laboratory studies.

In this study, we utilize results from geomechanical modeling to predict the seismic response to gas hydrate dissociation using common rock physics models. We "translate" the geomechanical model into seismic models. We estimate the sensitivity of seismic properties to a variation of input parameters to determine which parameters need to be particularly well calibrated in experimental and modeling studies. We then predict the seismic response from dissociating gas hydrates in 2-D using finite-difference (FD) wave-propagation modeling to demonstrate that despite the small predicted lateral extent of hydrate dissociation, its pronounced effect on seismic properties should allow detection with a seismic source on a drilling platform and receivers on the seafloor.

The many simplifications make this a conceptual study. However, it emerges that the most critical unknown for predicting the seismic response to gas hydrate dissociation seems to be the distribution of gas bubbles in the sediments.

SEISMIC ROCK PHYSICS MODELING

Methods

Most of this study is based on the predicted gas hydrate dissociation around a cased borehole [3] after 6.5 days (largely, Figure 5 in ref. [3]). Gas hydrate dissociation is modeled in a poro-elastic sand layer with a thickness much larger than the lateral extent of dissociation. The sediment has low permeability not allowing fluid flow within the several-day time-periods that were modeled. This assumption leads to significant pore pressure increase. The excess volume from gas hydrate dissociation into gas and water is accommodated by compression of free gas and by gas moving into solution.

Seismic properties of "reference" sediment: To predict seismic properties of the gas- and hydrate-free reference sediment, we used a deterministic approach based on the Hertz-Mindlin theory [6] as summarized by ref. [7], which predicts elastic properties of packed spheres. Porosity adjustment is achieved with Hashin-Shtrikman bounds [8].

Differential pressure, i.e., the difference between confining and pore pressure, is a critical parameter for Hertz-Mindlin-based models. The geomechanical model simulates a case with different horizontal and vertical stresses. Since our models do not account for anisotropic stresses, we used an average of the two horizontal stresses and the vertical stress as confining pressure since we think this is the best approximation of the force that "pushes" the spheres together in Hertz-Mindlin-based models.

We did not attempt to predict attenuation but used common values (quality factors for P- and S-waves of 200 and 25, respectively). We disregarded the likely increase of attenuation from the release of gas because the small gas-bearing patches are not thought to attenuate seismic waves significantly.

Addition of gas hydrates: Gas hydrates are added to the sediment model either as pore fill by using the Reuss average [9] between the properties of water and hydrate, or as load-bearing frame material [10]. For the latter, frame properties are calculated using the Hill-average [11] between grain and gas hydrate properties. Upper and lower bounds for frame properties are constrained using Hashin-Shtrikman bounds. Hydrate may also be present as cement between grain contacts or coating the grains. The seismic responses to both modes of cement are modeled using cementation models [12, 13].

Hertz-Mindlin-based models were found to be appropriate for predicting Vp in sands, based on laboratory measurements (e.g., ref. [14]) and also, for natural gas-hydrate-bearing sediments [10], although they tend to overestimate S-wave velocity (Vs) in unconsolidated natural sediments [15]. Our study however, focuses on Vp because its lowering by free gas is likely to have the most pronounced effect associated with gas hydrate dissociation.

We used a simplified cementation model that does not account for differential pressure [12]. For comparison of seismic models, we therefore focus on *changes* of seismic properties from cementation rather than absolute values. An alternative approach – to change grain properties for the cementation model such that properties of gas-hydrate-free sediments match those from Hertz-Mindlin-based models at a given differential pressure – led to a more pronounced increase of seismic velocities in the presence of hydrates than the models with correct grain properties. We don't think this is realistic: the higher the velocities of hydrate-free sediments the lower the velocity contrast between hydrates and bulk sediment. Hence, the increase of velocity should be less pronounced. Cementation models that accommodate differential pressure variations have recently been published [16].

Gas in porous media: The two extreme cases for gas distribution are either evenly distributed gas (i.e., all the pores contain gas at the same saturation) or "patchy" distribution for which a fractions of the bulk sediment are entirely gas saturated, whereas the remaining sediment is water saturated. Evenly distributed gas is modeled with the Biot-Gassman theory [17] by adjusting pore-fill properties using the Reuss average between water and gas properties, whilst patchy gas is modeled by calculating the Hill-average of the properties of gas- and water-saturated sediments [18]. The elastic properties of gas were determined using published approaches [19, 20] but accounting for a deviation of methane from an ideal gas [21].

The above approaches are established methods for estimating the properties of gas-hydrate- and gas-bearing sediments [10]. Resolution limits for wave-propagation modeling, combined with an almost total lack of calibration from laboratory or field experiments, did not allow us to include sediments *during* gas hydrate dissociation. Key parameters for seismic modeling are listed in Table 1. We used literature values for grain, gas hydrate, and water properties as summarized by refs. [10, 22].

Gas saturation as a function of initial gas hydrate saturation: Our geomechanical model does not account for fluid flow. It is thought that during the relatively short time spans of hydrate dissociation in low-permeability sediments, volume expansion from the release of gas during dissociation is accommodated by pore pressure, compressing gas bubbles, and by pushing gas into solution. The latter takes place because methane solubility increases when the hydrate stability field is exited [23] and also increases with pressure. In this case, gas saturation is determined by the volume made available during hydrate dissociation. Gas hydrate is less dense than water meaning one volume of s-I hydrate generates only 0.8 volumes of water. All the gas from dissociation would thus be "squeezed" into the newly created additional 0.2 volumes. In our case of a porosity of 0.5 and hydrate saturation of 0.5, gas saturation after dissociation is 0.1.

We also calculated the gas saturation from hydrate saturation assuming that pore-volume expansion is accommodated by single-phase fluid flow, i.e., both water and gas migrate, and gas saturation in the escaping fluids and that which remains in place are identical. In this case, we neglect the "loss" of methane gas that goes into solution due to an increase of methane solubility when pressure-temperature conditions leave the hydrate stability field. We note that in this scenario, the escaping gas will form hydrate and/or increase the partially gas-saturated region.

Parameters from geomechanical modeling	
Initial porosity	0.5
Initial gas hydrate saturation (1)	0.5
Confining pressure (2)	24.60 MPa
Initial pore pressure	15.87 MPa
Pore pressure after dissociation (3)	23.00 MPa
Temperature after dissociation (3)	292 K
Hydrate forming gas	Methane
Cage occupancy	100%
Seismic properties	
Compressional modulus – grain	37.0 GPa
Shear modulus – grain	44.0 GPa
Density – grain	2.650 g/cm^3
Compressional modulus – hydrate	7.70 GPa
Shear modulus – hydrate	3.21 GPa
Density – hydrate	0.910 g/cm^3
Compressional modulus – water	2.25 GPa
Density – water	1.035 g/cm^3
Coordination no.	9
Critical porosity	0.36

Table 1: Parameters used for seismic rock physics models
(1) Saturation as fraction of pore space
(2) Average between horizontal and vertical stresses
(3) Estimated average over entire region of dissociation

As another extreme, we estimated gas saturation of the pore space under the assumption that gas stays in place while water is expelled to accommodate volume expansion. We again neglect increased methane solubility. While this suggestion may at first be considered unrealistic, it is known that at low concentration, gas mobility in fine-grained sediments may be lower than that of water [24].

Results

Elastic properties of gas-hydrate-bearing sediments: Vp and Vs and their differences from velocities of gas-hydrate-free sediments as a function of gas hydrate saturation are shown in Figure 1. For a gas hydrate saturation of 0.5, Vp is predicted to increase by 2.07 km/s for grain-contact cementation, 0.50 km/s for the frame model (Hill average), and 0.28 km/s for the pore-fill model. Vs changes less dramatically in absolute terms, however from a much lower starting velocity. As density (ρ) remains almost constant, we do not show plots of the product of velocities and density, seismic impedances (I and J for P- and S-impedance, respectively).

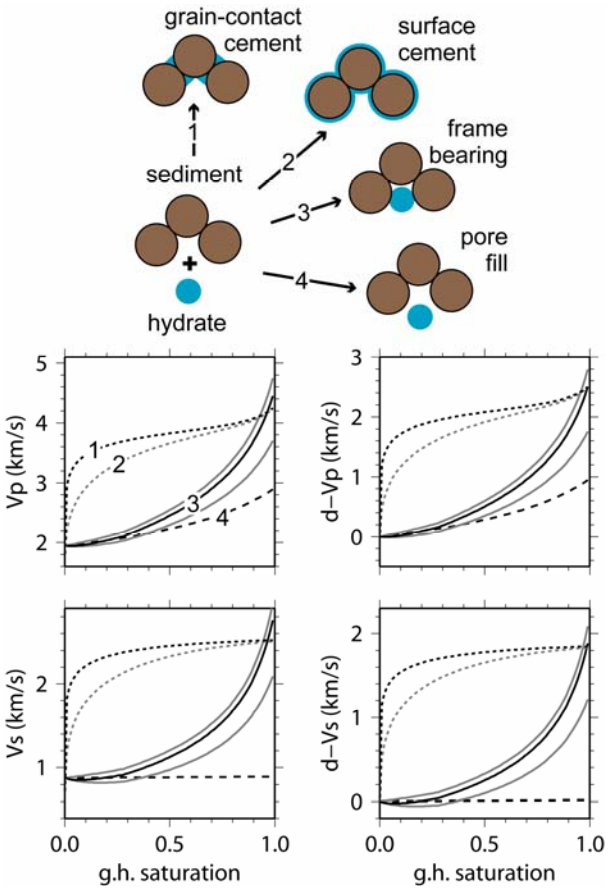

Figure 1: Velocities and their differences to gas-hydrate-free reference sediment as a function of hydrate saturation. Grey lines around the frame model mark Hashin-Shtrikman bounds. The differences are compared to the respective models for a gas hydrate saturation of zero.

Elastic properties of partially gas-saturated sediments: Because of the relatively high pore pressures, the decrease of Vp due to evenly distributed gas is not as pronounced as for ambient conditions [1] (Figure 2). Nevertheless, at saturations between ~0.05 and 0.3, the velocity differences between "patchy" and even distributions are ~0.7-0.8 km/s.

Pore pressure decreases seismic velocities. Sediments are overpressured after dissociation of hydrate to gas (23.00 MPa compared to 15.87 MPa before dissociation). Velocities are therefore lower than those of the reference sediment at full water saturation.

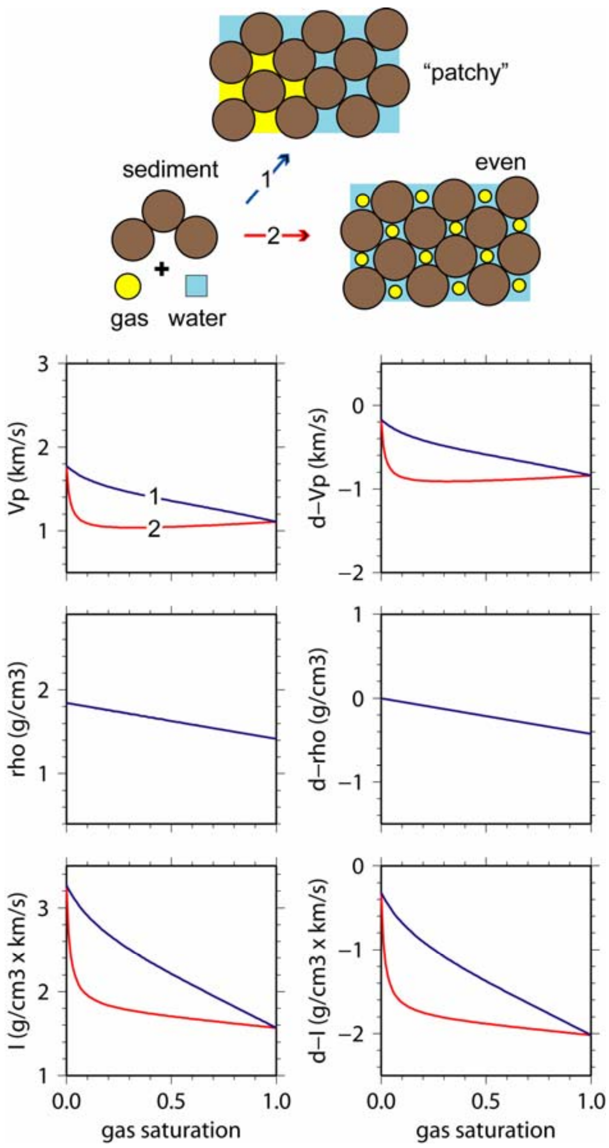

Figure 2: Vp, ρ, and I vs. gas saturation, assuming even and "patchy" distribution of gas bubbles in the pore space. Pore pressure is 23.00 MPa. The differences are calculated with respect to hydrate-free sediments at 15.87 MPa, hence the negative value at zero saturation.

Seismic reflection strength at near-vertical angles of incidence is controlled by contrasts in *impedance*, the product of density and velocity, not by velocity contrasts. Since density decreases with increasing gas saturation, impedance changes are more pronounced than velocity changes.

Gas saturation as a function of initial gas hydrate saturation: We estimated the sensitivity of velocity changes to some critical parameters. Since gas has a pronounced effect on Vp, models of gas hydrate dissociation need to accurately predict gas saturation in order to constrain seismic properties. We calculated gas saturation as a function of initial gas hydrate saturation for the three extreme scenarios of fluid flow outlined above (no flow, single-phase flow, and gas remaining in place). Pore pressure affects predicted gas saturation by compressing gas bubbles. As pore pressure is intuitively much lower if fluid flow takes place, we show in Figure 3 predicted gas saturation for hydrostatic pressure (15.87 MPa) and for 23.00 MPa. The differences between the three fluid-flow scenarios are significant. For the 23-MPa case, hydrate dissociation leads to gas saturation of 0.10 for the no-flow scenario, 0.27 for single-phase flow, and 0.34 if gas remains in place but water escapes. Gas saturations for 15.87 MPa case are even higher for the scenarios that allow fluid flow.

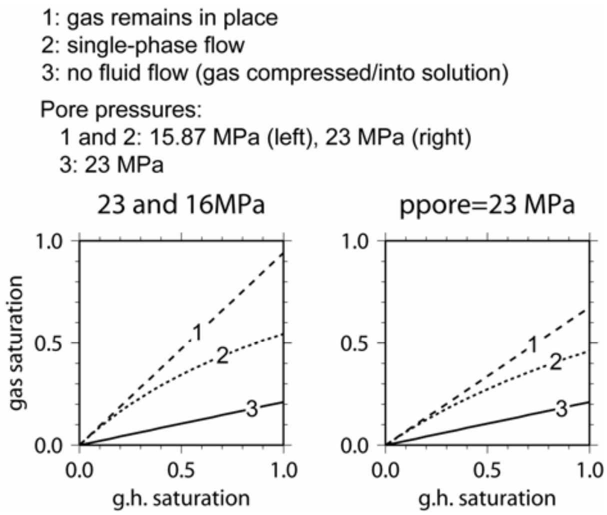

Figure 3: Gas saturation after dissociation as a function of original gas hydrate saturation. For the no-fluid-flow case, pore pressure is assumed to be 23.00 MPa in both panels.

Differences in P-wave properties are plotted against initial gas hydrate concentration assuming the three fluid-flow scenarios (Figure 4). The differences between the two models that allow fluid flow are not dramatic. However, gas saturation for the no-flow model is considerably lower than for the other two cases, leading to lower Vp.

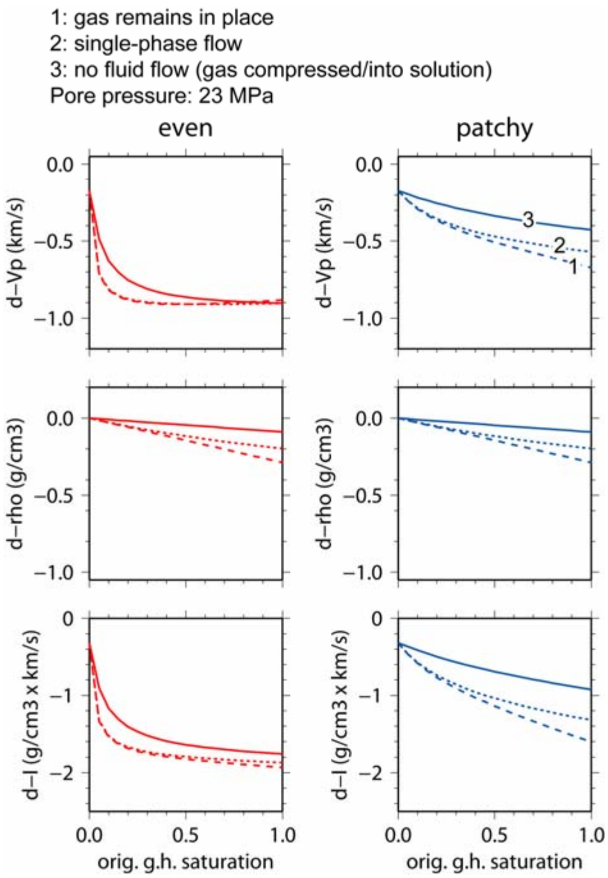

Figure 4: Differences in Vp, ρ, and I as a function of original gas hydrate saturation using the three fluid-flow scenarios shown in Figure 3.

Pore pressure: We have simulated the effect of pore pressure between hydrostatic and near-lithostatic pressure (Figure 5). Changes of both Vp and Vs from hydrostatic pressure (15.87 MPa) to the pore pressure predicted from geomechanical modeling (23.00 MPa) are in the order of -0.2 km/s (see also Table 2). The effect of pore pressure on elastic properties was dominated by the decrease of differential pressure, which pushes the spheres together, rather than a change of gas properties due to increased compression. Temperature (which affects gas properties) was found to be negligible within a realistic range.

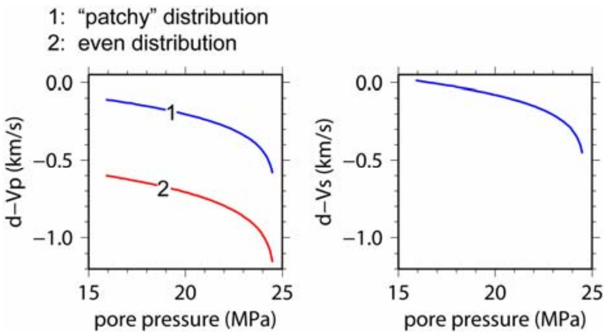

Figure 5: Velocity differences from reference values as a function of pore pressure. Hydrostatic pressure is 15.87 MPa, lithostatic 24.60 MPa.

Table 2 shows a summary of the most relevant findings.

Gas hydrate, saturation 0.5:				
	ΔVp	ΔI	ΔVs	ΔJ
Cement	2.07	6.91	1.78	3.20
Frame	0.50	0.84	0.24	0.41
Pore fill	0.28	0.45	0.24	0.41
Gas, initial hydrate saturation 0.5:				
	even		"patchy"	
	ΔVp	ΔI	ΔVp	ΔI
No flow	-0.77	-1.47	-0.34	-0.69
Single phase	-0.91	-1.79	-0.47	-1.03
Gas in place	-0.91	-1.82	-0.51	-1.06
Pore pressure variation (15.87-23.00 MPa):				
(no flow)	ΔVp	ΔI	ΔVs	ΔJ
15.87, even	-0.60	-1.16	0.01	0.02
"Patchy"	-0.11	-0.28	0.01	0.02
23.00, even	-0.77	-1.47	-0.21	-0.41
"Patchy"	-0.34	-0.69	-0.21	-0.41
Selected differences, Δ(ΔI)				
Gas hydrate: cement – pore fill				6.07
Gas, 23 MPa, no flow: "patchy" – even				0.78
Gas, even: no flow – gas in place				0.35
Gas, even: 15.87 – 23.00 MPa				0.31

Table 2: Key findings. Differences are compared to reference model (frame and pore-fill models at zero saturation, pore pressure 15.87 MPa), except for the cementation model.
Cement: Cementation between grain contacts
Frame: Hill-average of grain properties
Pore pressure for gas values is 23.00 MPa if not stated otherwise.

For an initial gas hydrate saturation of 0.5, the mode of hydrate distribution (here, grain contact cement compared to Hill-average frame model) has the strongest effect on P-impedance changes. However, we will point out in the discussion that such grain-contact cementation is probably not very common in natural settings. The difference between even and "patchy" gas distribution is second, followed by gas saturation and pore pressure.

FD WAVE-PROPAGATION MODELING

Method

Our rock physics models predict significant changes of elastic properties of sediments during gas hydrate dissociation. This is to be expected, independent of the type of rock physics models used, since it is well established that gas significantly lowers Vp [1]. However, the lateral extent of gas hydrate dissociation is miniscule compared to seismic wavelengths. Within the 6.5 days modeled by ref. [3], the gas hydrate dissociation front only moves ~1 m away from the borehole – total dissociation only occurs up to ~0.6 m (Figure 5 in ref. [3]).

Lateral resolution of seismic data has traditionally been defined by the first Fresnel zone, which depends on frequency, seismic velocities, source-to-target distance, and receiver-to-target distance [25]. In typical gas hydrate settings, the Fresnel zone is in the order of 10s to 100s of meters for a sea-surface source and seafloor receivers. On the other hand it is acknowledged that with adequate migration techniques, resolution can be much higher [26]. Resolution of migrated images depends largely on receiver spacing and aperture. Small targets with strongly contrasting elastic properties from their surrounding sediments constitute scatter points that cause diffraction hyperbolae before migration. These hyperbolae will be collapsed to point "reflections" during migration. The key is that while migration methods may not reproduce their exact geometry, these scatter points still will lead to detectable changes in the seismic records. Thus we here test whether our predicted contrasts in elastic constants may be sufficiently strong to allow detection of hydrate dissociation after 6.5 days, using the scenario of ref. [3].

A 2-D visco-elastic fourth-order staggered-grid FD approach [27] was used to simulate the seismic response to gas hydrate dissociation. We assumed a source on a platform above the borehole and seafloor receivers (Table 3) – this setup was thought to be practical for seismic monitoring because it allows frequent data acquisition without tying up expensive acquisition vessels (drilling and production would probably still need to be interrupted to decrease noise levels). We modeled wave propagation through the water column rather than "positioning" a source close the seafloor and "moving" the source to the sea surface by re-datuming the records in order to avoid artifacts that could adversely affect the relatively subtle diffraction hyperbolae. Most of our analysis focused on detecting diffraction hyperbolae from the assumed gas-bearing patches since development of such diffractions is likely to be the main indicator of gas hydrate dissociation. We only analyzed the pressure component of the seismic records.

Simulated acquisition geometry	
Receiver spacing	5 m
Source-receiver offset	± 1000 m
Source main frequency	70 Hz
Key modeling parameters	
Grid spacing	1 m
Model dimensions (width x depth)	3x2 km

Table 3: Key parameters for FD modeling, 6.5 days of dissociation [3], source at platform, seafloor receivers.

The use of 2-D models is a significant simplification. A 3-D version of the method would have required too much memory for the 1-m grid spacing used in our models. Strictly speaking, we simulate the response of a bar of dissociated hydrate stretching into the third dimension, rather than a patch. It is therefore likely we overestimate the response of gas hydrate dissociation around boreholes. In 3-D, this would be partly alleviated by using a 3-D receiver pattern. Additionally, staggered-grid methods are not ideally suited for modeling sharp property contrasts because implicitly, some "smearing" of properties occurs (some properties are calcualted for the edges, others for the centers of the grid elements – tests with other models using varying sampling rates however, did not reveal any significant differences). The purpose of FD modeling in this study is to investigate whether we would have any chance to detect gas hydrate dissociation a few days after its onset. Our findings from this conceptual study, that it is likely to be possible, should with caution still be applicable to the real-earth scenario.

Model

Background sediments: The gas-hydrate-bearing layer is located at 1563 m total depth, corresponding to hydrostatic pore pressure of 15.87 MPa [3]. Following the geologic scenario in ref. [3], we assumed a commonly used elastic-property-depth profile [28, 29] of sediments that were buried to 1765 m, corresponding to a vertical stress equal to the current maximum horizontal stress of 26.35 MPa. Sedimentation is followed by unroofing to current water depths of 1112 m, corresponding to the current vertical stress of 21.10 MPa. While arbitrary, these assumptions simulate over-consolidated sediments in the study area after which ref. [3] designed their models.

Gas-hydrate- and gas-bearing layer: A sand layer with properties as listed in Table 1 is inserted at 1558-1568 m (446-456 m beneath the seafloor). We set its thickness arbitrarily to 10 m. This is considerably larger than the lateral extent of gas hydrate dissociation, which was necessary to ensure the (cylindrical) 1-D constraint for the geomechanical models is accommodated (corresponding to infinite thickness of the hydrate layer). Furthermore, our goal was to test the *lateral* limits for detecting gas hydrate dissociation. Using thinner layers would seriously affect seismic images because of limited *vertical* resolution.
Grid-size limits did not allow sufficiently dense sampling to include the borehole in our modeling. To model gas-bearing sediments, we inserted a patch of 1-m lateral (mimicking gas hydrate dissociation ±0.5 m away from the borehole), 10-m vertical extent. The resulting Vp-profile is shown in Figure 6a.

Seismic source and noise: The synthetic seismic traces were modeled based on ocean-bottom-seismometer (OBS) records acquired to study gas hydrates in similar water depths on Hydrate Ridge [30]. We used a source signal with a similar main frequency (70 Hz, Ricker wavelet) and added noise with similar amplitudes and frequencies (Figure 6b). The resulting record (Figure 7a) appears like a "real" dataset (upon closer inspection we noticed that the low-frequency noise in the OBS data, which is probably caused by wave energy and/or rocking of the instrument in ocean currents, is more coherent than the Gaussian noise added to the synthetic data).

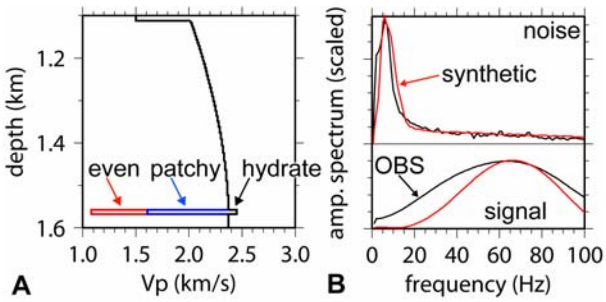

Figure 6: A: Vp vs. depth used in modeling (Figure 7), even and patchy gas saturation close to borehole, gas hydrate further away from borehole.
B: Top: Noise spectrum of OBS data obtained from energy above the direct arrival compared to that after adding noise to synthetic data. Bottom: Signal spectrum from a window around the direct arrival. Both sources have similar main frequencies although the spectrum of the real data is broader.

Apart from a broad bandpass filter (Butterworth 8/16-120/160 Hz), the synthetic data in Figures 7b-7d are not processed. A diffraction hyperbola is clearly present above the noise level in the case of evenly distributed gas (Figure 7b). Some traces of a diffraction are also present for patchy distribution (Figure 7c). Using a noise level of $1/10^{th}$ of that of the OBS data, the diffraction becomes much more obvious. The noise level could for example be reduced by repeated shooting (although for a reduction by a factor of 10, 100 shots would be required). Also, buried geophones are likely to be much less noisy than OBSs deployed at the seafloor. For comparison, the radius of the Fresnel zone for this configuration would be ~90 m.

Surface seismic after 1 year of dissociation

Gas hydrate dissociation may pose a problem during the entire lifespan of an oilfield. Ref. [2] modeled gas hydrate dissociation around boreholes over 1-30 years. We used results from their 1-year model to test whether gas hydrate dissociation would be likely to be recognized in “conventional” 4-D surveys with surface seismic. For this model, we used a the porosity-depth function in their 2-D system (Table 3 in ref. [2]) and inserted a hydrate layer using the properties of their reference case

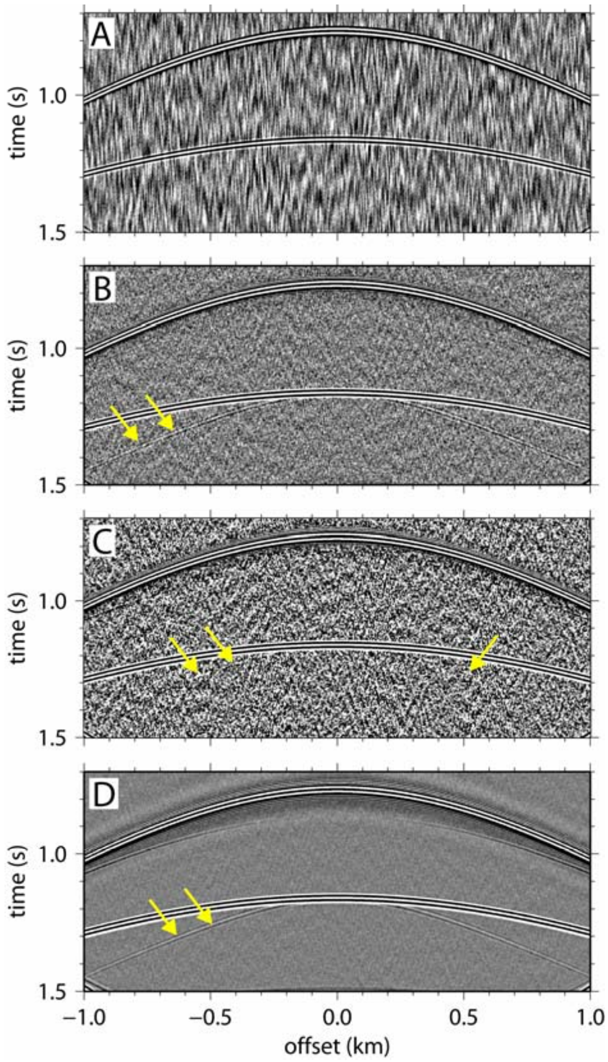

Figure 7: Synthetic seismograms from FD modeling. Plots are scaled to the strength of the direct arrival.
A: Unfiltered reference section before gas hydrate dissociation. Amplitude scaling: 100x maximum of direct arrival.
B: Dissociation, even distribution of gas in pores. Amplitude scaling: 200x maximum of direct arrival. Arrows: Diffraction hyperbola from gas after hydrate dissociation.
C: Dissociation, “patchy” distribution of gas in pores. Amplitude scaling: 2000x maximum of direct arrival. Fragments of a diffraction can be identified (mostly, in larger-scale plots).
D: Dissociation, “patchy” distribution of gas in pores, noise level $1/10^{th}$ of that in OBS. Amplitude scaling: 500x maximum of direct arrival.

(Table 1 in ref. [2]), however with 10-m rather 1-m thickness. We realize that the latter will affect in particular pressure distribution and thus, ignored overpressure, lowering the seismic response to gas hydrate dissociation. A 4-m dissociation radius was assumed around the borehole, i.e., an 8-m wide, 10-m thick patch, and even distribution of gas (Figure 8a).

We simulated a two-ship survey to "undershoot" the platform, with one vessel towing a seismic streamer and the other an airgun array on the opposite side of the platform. Both receivers and sources approached the borehole up to 500 m. Critical input and acquisition parameters are listed in Table 4. After adding realistic noise, based on visual comparison to real streamer data, simple standard processing was performed (common-mid-point sorting, velocity analysis, normal-moveout correction, stacking, post-stack migration). Note that we did not take advantage of knowing the velocity-depth function which in reality would be well known. The resulting plots (Figure 8) clearly show a seismic response to gas hydrate dissociation. As expected, lateral resolution thwarts the image by stretching it over about ten times the actual lateral extent of dissociation; however, a seismic signal from dissociation would be detected. We did not model "patchy" saturation given the significant computing time (48 shots) but we are confident that it would be recognized too, considering the strong signature from even gas distribution (with 0.31, the overall gas saturation is higher than for the first case; hence, the velocity decrease is more pronounced for "patchy" distribution).

DISCUSSION

Our rock physics modeling shows that the difference between grain-contact cementation and frame or pore models has the strongest effect on changes in elastic properties, particularly P-impedance. However, cementation in this sense is not thought to occur often in nature. Vp in gas-hydrate bearing sediments from the Mallik boreholes [15] congregates around frame models. We caution that gas hydrates formed in sediments in the laboratory sometimes does appear to cement grains [31, 32]. In real-life scenarios, we would assume some a-priori information to be available, such as resistivity and sonic logs that would probably allow detection of hydrate cementation.

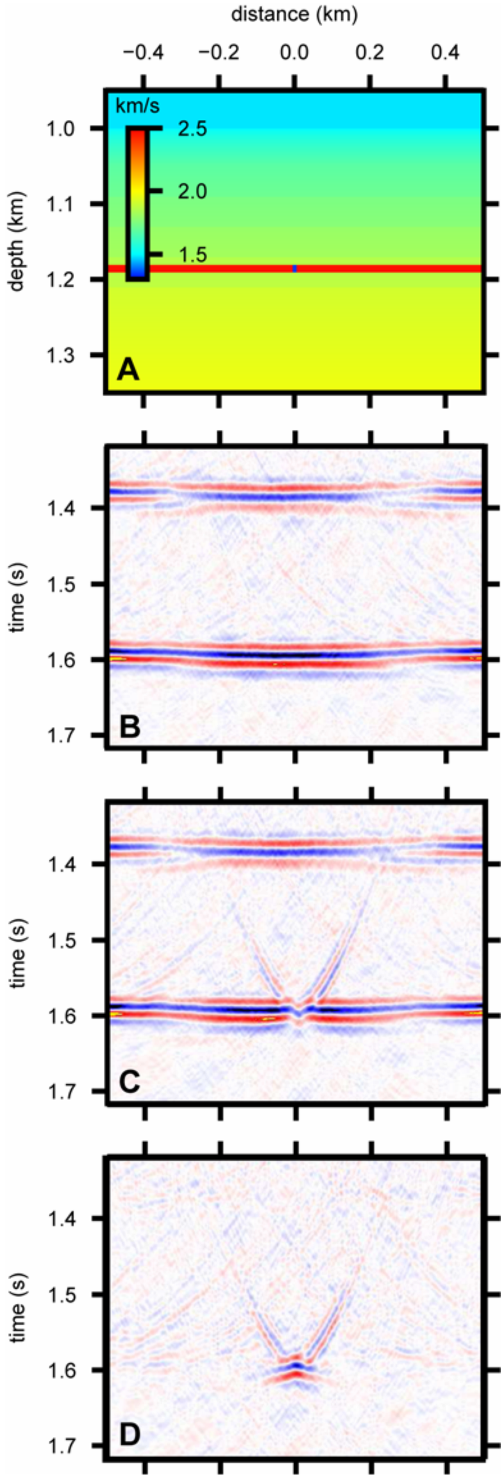

Figure 8: Modeling the response in surface-towed data to gas hydrate dissociation after 1 year.
A: Velocity model, even distribution of gas
B: Gas hydrate layer before dissociation at ~1.6 s, amplitudes scaled to reflection from this layer
C: After gas hydrate dissociation
D: Difference plot

Parameters from geomechanical modeling	
Porosity	0.3
Initial gas hydrate saturation	0.5
Gas saturation after dissociation (1)	0.31
Pore pressure (2)	11.95 MPa
Confining pressure (3)	13.49 MPa
Temperature (2)	286 K
Seismic properties – as in Table 1 except for:	
Density – grain (1)	2.750 g/cm^3
Simulated acquisition geometry	
Receiver spacing	10 m
Maximum source-receiver distance	2500 m
Shot spacing	20 m
Minimum distance to platform	500 m
Source main frequency	50 Hz
Key modeling parameters	
Grid spacing	2 m
Model dimensions (width x depth)	3x1.5 km

Table 3: Key parameters for FD modeling, 1 year of dissociation [2], surface seismic, two-ship experiment.
(1) From ref. [2]
(2) Changes of pore pressure and temperature not accounted for
(3) Calculated from Table 3 in ref. [2] and pore pressure

The mesoscopic distribution of gas (even or "patchy") is the next significant factor for the seismic response to hydrate dissociation, followed by gas saturation. Geomechanical models need to predict how much gas will be generated and how of it much escapes. Gas saturation needs to be particularly well constrained for "patchy" distribution because Vp is more sensitive to "patchy" gas pockets at intermediate saturations than to evenly distributed gas (see e.g., Figure 2). Geomechanical models also need to predict pore pressure which has significant effects on seismic properties.
Laboratory studies and information from field data will calibrate rock physics models. Laboratory studies are in particular important for studying the response to gas hydrate formation and dissociation with the two caveats that hydrate formation may not mimic that in nature, potentially leading to different seismic responses. Results from ultrasonic measurements also have limited applicability for the seismic frequency range [33].

Because of the limited resolution of our FD models, we did not attempt to model the seismic response to sediments *during* gas hydrate dissociation, when gas and hydrate co-exists. However, we note that a relatively large region is in the process of dissociation for the 6.5-day model by ref. [3]. We speculate that two effects are particularly significant. It needs to be studied when gas hydrates lose grain contact. We also need to know when the released gas is seismically connected to the remaining pore space, which is a pre-requisite for any significant seismic response to the presence of gas in the pores.
Constraining most of the above unknowns is a fairly common problem in reservoir monitoring. The big exception however is a determination of the mesoscopic distribution of gas in the sediment pores. Gas may occur in "patches" of several meters making laboratory studies difficult. Furthermore, gas pockets may re-arrange over time after dissociation. Anecdotal evidence suggests that P-wave signals in the laboratory "bounced back", i.e., became stronger and arrived slightly earlier some time after dissociation (Winters, pers. comm. 4/2008; Yang, pers. comm. 4/2008) consistent with re-alignment of gas bubbles into "patchier" distribution.
Our FD modeling suggests that seismic time-lapse monitoring of gas hydrate dissociation should be feasible, depending on the required time scales: While it will be challenging to detect the onset of gas hydrate dissociation after only a few days, gas hydrate dissociation should be recognized after 1 year even in "conventional" surveys. We realize that our FD modeling is simplified. The 2-D approach and the simple, essentially 1-D velocity structure may increase the signature of gas hydrate dissociation in real sediments. On the other hand, we did not use any sophisticated processing strategies for the synthetic data. For real data, velocity information would probably exist from vertical seismic profiles. Noise in buried receivers should be considerably lower than that in OBSs. Repeat shooting would also decrease the noise level. Different survey designs could also be considered, e.g., involving a source close to the seafloor or permanently installed borehole receivers.

Conclusions

Our study suggests the key factors for predicting the seismic response of sediments to hydrate dissociation are the mode of gas hydrate distribution (in particular, contact cement vs. frame bearing), gas distribution in the sediments (even vs. "patchy"), gas saturation, and pore pressure. FD modeling shows that gas hydrate dissociation may be recognized after several days using monitoring with seafloor receivers and a source on the drilling platform. The most challenging parameter for designing monitoring systems and assessing their sensitivities is likely to be the mesoscopic distribution of gas in sediments.

ACKNOWLEDGMENTS

We would like to thank T. Bohlen for making the FD modeling code available to us.

REFERENCES

[1] Domenico SN. *Elastic properties of unconsolidated porous sand reservoirs.* Geophysics 1977;42:1339-1368.

[2] Moridis GJ, Kowalsky MB. *Response of oceanic hydrate-bearing sediments to thermal stresses*. *In: Proceedings 2006 Offshore Technology Conference*. Houston, TX, 2006.

[3] Freij-Ayoub R, Clennell B, Tohidi B, Yang J, Hutcheon R. *Casing integrity in hydrate bearing sediments*. *In: Proceedings 6th Intl. Offshore Site Investigation and Geotechnics Conf.* London, 2007.

[4] Freij-Ayoub R, Tan C, Clennell B, Tohidi B, Yang J. *A wellbore stability model for hydrate bearing sediments.* J. Pet. Sci. Eng. 2007;57:209-220.

[5] Yang J, Tohidi B, *Geophysical properties and dynamic response of methane hydrate-bearing sediments to hydrate formation and decomposition*. In: S. Chopra et al., editor Gas Hydrates. Society of Exploration Geophysicists, submitted.

[6] Mindlin RD. *Compliance of elastic bodies in contact.* Trans. SDME 1949;71:259-268.

[7] Mavko G, Mukerji T, Dvorkin J. *The Rock Physics Handbook*, Cambridge, U.K.: Cambridge University Press, 1998.

[8] Hashin Z, Shtrikman S. *A variational approach to the elastic behavior of multiphase materials.* J. Mech. Phys. Solids 1963;11:127-140.

[9] Reuss A. *Berechnung der Fliessgrenze von Mischkristallen.* Zeitschrift fuer Angewandte Mathematik und Mechanik 1929;71:259-268.

[10] Helgerud MB, Dvorkin J, Nur A, Sakai A, Collett T. *Elastic-wave velocity in marine sediments with gas hydrates: effective medium modeling.* Geophys. Res. Lett. 1999;26:2021-2024.

[11] Hill R. *The elastic behavior of crystalline aggregate.* Proc. Phys. Soc. London 1952;A65:349-354.

[12] Dvorkin J, Nur A. *Elasticity of high-porosity sandstones: Theory for two North Sea data sets.* Geophysics 1996;61:1363-1370.

[13] Ecker C, Dvorkin J, Nur A. *Sediments with gas hydrates: Internal structure from seismic AVO.* Geophysics 1998;63:1659-1669.

[14] Prasad M, *Experimental and theoretical considerations of attenuation and velocity interactions with physical parameters in sands*, in *Institute of Geophysics*. 1988, University of Kiel: Kiel, Germany. 123.

[15] Lee MW. *Elastic properties of gas hydrate-bearing sediments.* Geophysics 2001;66:763-771.

[16] Leurer K, Dvorkin J. *Viscoelasticity of precompacted unconsolidated sand with viscous cement.* Geophysics 2006;71(2):T31-T40.

[17] Gassmann F. *Ueber die Elastizitaet poroeser Medien.* Vierteljahreszeitschrift der Naturforschenden Gesellschaft in Zuerich 1951;96:1-23.

[18] Dvorkin J, Moos D, Packwood JL, Nur A. *Identifying patchy saturation from well logs.* Geophysics 1999;64:1756-1759.

[19] Gray DE, editor. *American Institute of Physics Handbook.* 3rd ed. 1972, McGraw-Hill, New York.

[20] Parker SP, *McGraw-Hill dictionary of scientific and technical terms*. New York: McGraw-Hill, 1989.

[21] Duan Z, Moeller N, Weare JH. *An equation of state for the CH4-CO2-H2O system. I. Pure systems for 0 to 1000 C.* Geochim. Cosmochim. Acta 1992;56:2605-2617.

[22] Waite WF, Helgerud MB, Nur A, Pinkston J, Stern LA, Kirby SH, Durham WB, *First measurements of P- and S-wave speed on pure methane gas hydrate.* Suppl. to Eos, 10 Nov. 1998, AGU Fall Meeting. 1998. p. 463.

[23] Zatsepina Y, Buffett BA. *Phase equilibrium of gas hydrate: Implications for the formation of hydrate in the deep sea-floor.* Geophys. Res. Lett. 1997;24:1567-1570.

[24] Honarpour M, Koederitz L, Harvey AH. *Relative permeability of petroleum reservoirs*, Boca Raton, FL: CRC Press, 1986.

[25] Yilmaz Ö. *Seismic data analysis*. 2 ed. Investigations in Geophysics, Doherty SM. Vol.

10, Tulsa, OK: Society of Exploration Geophysicists, 2001.

[26] Chen J, Schuster GT. *Resolution limits of migrated images.* Geophysics 1999;64:1046-1053.

[27] Bohlen T. *Parallel 3-D viscoelastic finite difference seismic modelling.* Comp. Geosci. 2002;28:887-899.

[28] Hamilton EL. *Sound velocity-density relations in sea-floor sediments and rocks.* J. Acoust. Soc. Am. 1978;43:366-377.

[29] Hamilton EL. *Variations of density and porosity with depth in deep-sea sediments.* J. Sediment. Petrol. 1978;46(2):280-300.

[30] Bangs NL, Pecher IA, Ewing Leg EW0208 Science Party. *Shear wave studies of Hydrate Ridge, Oregon margin; R/V Ewing and JOIDES Resolution Seismic Experiments.* Austin: University of Texas, 2002.

[31] Waite WF, Winters WJ, Mason DH. *Methane hydrate formation in partially water-saturated Ottawa sand.* Amer. Miner. 2004;89:1202-1207.

[32] Winters WJ, Pecher IA, Waite WF, Mason DH. *Physical properties and rock physics models of sediment samples containing natural and laboratory-formed methane gas hydrate.* Amer. Miner. 2004;89:1221-1227.

[33] Batzle ML, Han D-H, Hoffmann R. *Fluid mobility and frequency-dependent seismic velocity - Direct measurements.* Geophysics 2006;71:N1-N9.